Published in final edited form as:
*Nano Lett*. 2011 April 13; 11(4): 1477–1482. doi:10.1021/nl1040836.

# Stability of DNA Origami Nanoarrays in Cell Lysate

**Qian Mei**[†], **Xixi Wei**[‡,§], **Fengyu Su**[†], **Yan Liu**[‡,§], **Cody Youngbull**[†], **Roger Johnson**[†], **Stuart Lindsay**[‡,§,‖], **Hao Yan**[‡,§,*], and **Deirdre Meldrum**[†,*]

[†]Center for Biosignatures Discovery Automation, Arizona State University, Tempe, Arizona 85287, United States

[‡]Center for Single Molecule Biophysics, Arizona State University, Tempe, Arizona 85287, United States

[§]Department of Chemistry and Biochemistry, Arizona State University, Tempe, Arizona 85287, United States

[‖]Department of Physics, Arizona State University, Tempe, Arizona 85287, United States

## Abstract

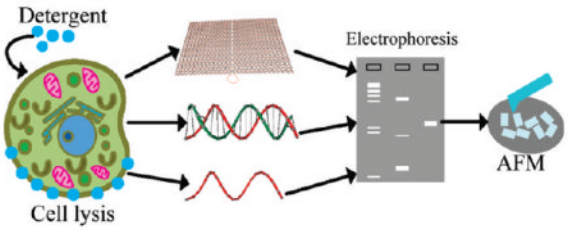


Scaffolded DNA origami, a method to create self-assembled nanostructures with spatially addressable features, has recently been used to develop water-soluble molecular chips for label-free RNA detection, platforms for deterministic protein positioning, and single molecule reaction observatories. These applications highlight the possibility of exploiting the unique properties and biocompatibility of DNA nanostructures in live, cellular systems. Herein, we assembled several DNA origami nanostructures of differing shape, size and probes, and investigated their interaction with lysate obtained from various normal and cancerous cell lines. We separated and analyzed the origami–lysate mixtures using agarose gel electrophoresis and recovered the DNA structures for functional assay and subsequent microscopic examination. Our results demonstrate that DNA origami nanostructures are stable in cell lysate and can be easily separated from lysate mixtures, in contrast to natural, single- and double-stranded DNA. Atomic force microscope (AFM) and transmission electron microscope (TEM) images show that the DNA origami structures are fully intact after separation from cell lysates and hybridize to their targets, verifying the superior structural integrity and functionality of self-assembled DNA origami nanostructures relative to conventional oligonucleotides. The stability and functionality of DNA origami structures in cell lysate validate their use for biological applications, for example, as programmable molecular rafts or disease detection platforms.



[*]Corresponding Author: Deirdre.Meldrum@asu.edu, Hao.Yan@asu.edu.

ASSOCIATED CONTENT

Supporting Information. Experimental methods, DNA sequences, electrophoretic gel images, and microscopy images. These materials are available free of charge via the Internet at http://pubs.acs.org.

**Keywords**

DNA origami; structural DNA nanotechnology; biocompatibility; self-assembly

Scaffolded DNA origami is a relatively new technique that uses hundreds of short “staple” DNA oligonucleotides to direct the folding of a single-stranded DNA scaffold, typically the 7249 nucleotide (nt) long M13 viral DNA genome, into a predefined structure.[1–3] This is an attractive method to construct nanoscale objects because of the ease and convenience of design, low production cost, high assembly yield, and unparalled addressability of the resulting origami structures. Many 2D[1] and 3D nanoarchitectures[4–8] assembled by this technique have been used to pattern various materials, serve as nanoscale rulers for single molecule imaging,[9] act as platforms for molecular robotics,[10] and observe single molecule chemical reactions.[11] In addition to these purposes, the distinctive properties of DNA origami structures make them particularly interesting for potential biological applications. The size of DNA origami nanostructures, the existence of well developed chemistries and enzymatic methods to modify their nucleotides and functionalities, and their biocompatibility permit their use in cellular studies. DNA origami has already been used as an addressable support to place proteins at precise positions and intermolecular distances,[12–14] and for label-free detection of RNA hybridization, which suggests a potential to assay for gene expression at the single molecule level.[15] Most recently, Seeman and co-workers[16] developed an elegant strategy to use DNA origami as a molecular chip to detect single nucleotide polymorphism (SNP), further demonstrating the potential of DNA nanostructures for biological applications. With the developments in high-speed atomic force microscopy (AFM)[17,18] and super-resolution fluorescence imaging,[19] DNA origami nanostructures are more readily characterized, further encouraging their utilization in single cell studies.

Though significant progress has been made over the past several decades in single cell proteomic analysis, most new methods are performed as end point analyses and provide only a snapshot of cell status. These problems are exacerbated by the low abundance of rare proteins and disease markers, whose presence is often difficult, if not impossible, to detect. With DNA origami, it may be possible to develop a platform that can be used for single, live cell analysis, with sufficient sensitivity to provide an accurate picture of intracellular dynamics. Microfluidic technologies for mixing,[20–23] in situ cell lysis[24–29] and subsequent electrophoretic separation[30–33] of cellular components have recently been developed by several research groups. It is our goal to apply the latest technologies to construct a microfluidic device consisting of a mixing chamber, lysis chamber, and electrophoretic channel to analyze cell-integrated, DNA origami platforms for cellular analysis. However, before DNA origami can be used to probe real-time cellular behavior, or as a disease detection or diagnosis tool, several issues must be addressed. For example, it is well-known that oligonucleotides may be unstable and easily degraded in cellular environments.[34,35] Therefore, it is critical to establish the stability of DNA origami structures in intra- and extracellular environments and determine whether or not they can be separated intact from cell lysate.

Here we investigated the stability of a series of DNA origami structures in cell lysates from a number of normal and cancerous cell lines and their ability to be separated from the cell lysate mixtures (Figure 1). The concentration of cells used to prepare the lysate (and therefore the amount of enzymes and other cellular material) was varied, along with DNA structure/lysate incubation time and temperature to determine if the DNA origami structures were stable under a wide variety of conditions. Several well-studied, 2D and 3D DNA origami nanostructures were assembled and purified following published methods.[1,7] Cell

lysate was prepared by mixing cells with mammalian cell lysis buffer (50 mM Tris-HCl, 150 mM NaCl, 0.1% SDS, 0.5% deoxycholic acid and protease inhibitor), followed by centrifugation to remove nuclear DNA and cell membrane debris. After the purified DNA origami structures were incubated with cell lysate, separation was performed by nondenaturing agarose gel electrophoresis. The morphological integrity of the structures was verified by direct visualization with AFM and transmission electron microscopy (TEM).

First, the stability of the same 2D, rectangular origami (90 nm × 60 nm) that was reported for label-free detection of RNA hybridization[15] was investigated. The rectangular origami was added to CP-A cell lysate (metaplastic human esophageal epithelial cell line[36]) prepared from different numbers of cells (5000 or 10000) and was subsequently incubated for 1 or 12 h at 4 °C or room temperature, respectively. Native gel analysis of each reaction mixture is shown in Figure 2a. For each gel, lane 1 contains a 1000 bp DNA ladder, used as a marker to identify the molecular size of each band, while lanes 2 and 3 and 6 and 7 contain the DNA origami/cell lysate mixtures corresponding to the various conditions. Lane 4 contains a DNA origami sample (not mixed with cell lysate), used as a positive control to illustrate the mobility of a fully formed structure, while lane 5 contains a sample of cell lysate only, as a negative control. In lanes 2, 3, 6, and 7, the presence of a band with the same mobility as the DNA origami control in lane 4 confirms that the DNA origami structures are stable in each of the conditions and can be successfully separated from cell lysate mixtures.

The relative intensity of each band was quantified using ImageJ, and the concentration of DNA origami structures in the bands separated from the cell lysate was estimated by comparison to the intensity of the band of the positive control (Figure 2b). No significant differences were observed for the various conditions. It should be noted that the intensities of the origami bands from the 25 °C reactions were approximately 98% of those from the 4 °C reactions. This result suggests that the DNA origami–cell lysate mixtures are stable at room temperature, obviating the requirement for any cooling device in the future design of a microfluidic chip.

To further verify their structural integrity and degree of separation from the cell lysate, DNA origami structures were extracted from the gels and visualized by AFM. The AFM images in Figure 2c and Figure S1 (Supporting Information) clearly show the rectangular DNA origami structures have been separated from the cell lysate, remaining fully intact with no evidence of degradation. For comparison, a mixture of DNA origami and cell lysate (no electrophoretic separation) was directly deposited on a mica substrate for AFM readout. Figure 2d shows that individual DNA origami structures cannot be identified in AFM images of the mixtures with cell lysate, because broken lipid membranes, proteins, nucleic acids and cellular organelle debris obscure the nanostructures. The cell remnants adsorb to the mica surface, preventing the DNA origami structures access to the substrate. Cell lysate constituents may also adsorb to the AFM tip while scanning, reducing image quality. These results confirm that separation, electrophoretic or otherwise, is a critical step for AFM analysis of DNA origami/cell lysate mixtures.

In the future, other 2D and 3D DNA origami structures may be required for tailored applications. It is therefore desirable to determine whether the shape of a structure has any influence on its stability in, or separability from, cell lysate. Two additional DNA origami constructions, whose shape and helical density might be presumed to affect their susceptibility to enzyme digestion, were investigated: a 2D equilateral triangle (120 nm long with 30 nm wide sides) with an open, central, triangular cavity of 60 nm per side and a 3D multilayer rectangular parallelepiped structure (8 helix × 8 helix square lattice with dimensions of 16 nm × 16 nm × 30 nm). The triangular and cuboid structures were prepared, mixed with CP-A cell lysate, and separated by gel electrophoresis (Figure 3a). The results

show that both additional DNA origami shapes can be separated from CP-A cell lysate, with no significant damage to the structures. A small amount of the triangular DNA origami structure remained in the wells, reflecting the known tendency of these structures to self-associate by base-stacking at the corner to form larger aggregates. The structures were subsequently extracted from the gels and imaged using AFM and TEM, as shown in panels b and c of Figure 3, respectively. The results indicate that regardless of size or shape, DNA origami structures are stable in, and separable from, a variety of cell lysate mixtures under the investigated conditions. The ability of these synthetic DNA structures to resist association with any cellular components and degradation by the DNA enzymes in the cell lysate might not have been predicted, considering how readily native DNA (both single stranded and double stranded) can interact with various DNA binding proteins and be digested in the intracellular environment. It is possible that the cellular machinery and enzymes do not recognize DNA in an origami structure as they normally would, or perhaps cannot access it given the relatively compact arrangement of DNA helixes due to limited steric accessibility. In addition, origami structures have a very high negative charge density, which may contribute to the inaccessibility of cellular components and enzymes to DNA origami surfaces.

To determine the interaction of cell lysate with traditional DNA and compare the results to those of DNA origami structures, representative single- and double-stranded DNA were also tested. It was expected that the natural, noncompact structure of single- and double-stranded DNA should be less resistant to interaction with, and degradation by, the components in cell lysate. M13mp18 viral DNA, which acts as the scaffold strand in the assembly of DNA origami, was selected as the representative single-stranded DNA; $\lambda$ DNA, ~47 kbp from *E. coli*, was used as the double-stranded DNA. Mixtures of single-and double-stranded DNA with cell lysate were prepared in the same way as the rectangular DNA origami–lysate mixture. After 1 or 12 h of 25 °C incubation in CP-A lysate, only the DNA origami remained unchanged as shown in the gel images in Figure 4. Notably, after only 1 h of incubation with cell lysate, comparing the gels from the untreated and treated samples, the single-stranded M13 mp18 viral DNA and double-stranded $\lambda$ DNA were completely altered, as evidenced by the disappearance of their representative bands. After treatment with cell lysate, the single-stranded DNA did not run as a single band but was smeared throughout the lane: the appearance of products with smeared faster mobility indicates that some of the single-stranded DNA was digested by cellular enzymes; the products with smeared slower mobility indicate severe protein binding and maybe some degradation. In the case of $\lambda$ DNA, nearly the entire sample of double-stranded DNA remained in the gel well. It is likely that the double-stranded DNA was interacting with some component in the cell lysate, possibly becoming entangled with cellular proteins. DNA origami is better able to maintain its integrity in cell lysate compared to single- and double-stranded DNA, likely because the rigidity, compact organization, and charge density of the origami structure decrease its susceptibility to degradation and propensity to interact with lysate components.

Cell-line-dependent effects of lysate on the stability and separation of DNA origami structures were also investigated. Normal End1/E6E7, MCF-10A and cancerous HeLa & MDA-MB-231 cells (see detailed description in Supporting Information) were lysed and separately mixed and incubated with DNA origami, double-stranded $\lambda$ DNA, and single-stranded M13mp18 viral DNA. Figure S2 (Supporting Information) shows the results of agarose gel separation of the mixtures, with each cell line exhibiting similar patterns to those of the CP-A cell lysate experiments. No notable cell line dependent effects were observed, and the results confirm that only the folded structure of DNA origami is stable in the various cell lysates. Most of the double-stranded $\lambda$ DNA remained in the wells when mixed with the cell lysates, possibly because of entanglement with proteins in the lysate mixture.

Finally, to confirm the functionality of DNA origami with interaction of cell lysate, a region of human *β*-actin gene (40 bases long) was linked as a capture probe onto the rectangular-shaped origami and then mixed with HeLa cell lysate. Twelve copies of probe were aligned into each strand on the right edge of the origami, while a sequence not found in the human genome was selected as a control and located at the same position as the probe (Figure S6, Supporting Information). Six of the dumbbell-shaped structures were placed on the upper left corner as index feature to orient the image, as described previously.[15] Detailed sequences of the probe, control, and index can be found in the Supporting Information (Table S4). After 1 and 12 h room temperature incubation with lysate prepared from various numbers of cells, origami with a capture probe was successfully separated from cell lysate as shown in Figure 5a. The gel images show that DNA origami/probe is still separable from the lysate, even after 12 h of incubation. The origami bands were cut from the gel for further functional assay. First synthetic RNA with complementary sequence to the probes (40 bases) was reacted with probe origami. AFM images of hybridized origami, such as in Figure 5c, revealed that the target hybridization can be visualized as bright features along the line of the probes, while no such binding was evident on the control (Figure 5b). Two more targets, fragmentized total cellular RNA and total cellular RNA, were prepared and reacted with probe-bearing origami after recovering from cell lysate. Those total cellular RNA should contain the mRNA for *β*-actin gene that is complementary to the probes. The AFM images of panels d and e of Figure 5 confirmed the obvious hybridization between probe origami and total cellular RNA, but no target binding on the control probe line as shown in panels b and c of Figure S7 (Supporting Information). Excess total cellular RNA was observed as aggregated dots on the mica surface (Figure 5e and Figure S7c (Supporting Information)). These results indicate that the single-stranded probes are not digested by cellular enzymes and remain functional for RNA hybridization after exposure to the cell lysate even for 12 h.

In summary, we have demonstrated the successful electrophoretic separation of a variety of DNA origami nanostructures from the lysates of several cell lines. The structural integrity of the resulting DNA origami was verified by AFM and TEM imaging, confirming that the structures can be separated from cell lysate without degradation or damage. We also established that DNA origami structures are stable in lysate mixtures for at least 12 h at room temperature, in contrast to natural, single- and double-stranded DNA configurations. Finally, we confirmed that DNA probe origami is not only stable but also functional after extended exposure to cell lysate. These results imply that DNA origami should remain stable in intracellular conditions and has the potential to serve as an in vitro diagnostic platform. Collectively, the experimental results encourage the development of an integrated, microfluidic chip for origami separation after cell lysis. This type of integrated device could be used for single cell proteomic analysis and provide sufficient sensitivity to ascertain an accurate picture of intracellular dynamics.

## Supplementary Material

Refer to Web version on PubMed Central for supplementary material.

## Acknowledgments

This work is supported by NIH Grant Number R01GM088818 from The National Institute of General Medical Sciences (NIGMS). We would like to thank Ms. Patti Senechal-Willis for cell culture.

## References

1. Rothemund PWK. Nature. 2006; 440:297. [PubMed: 16541064]
2. Kuzuya A, Komiyama M. Nanoscale. 2010; 2:310. [PubMed: 20644813]

3. Nangreave J, Han D, Liu Y, Yan H. Curr Opin Chem Biol. 2010; 14:608. [PubMed: 20643573]
4. Douglas SM, Dietz H, Liedl T, Hogberg B, Graf F, Shih WM. Nature. 2009; 459:414. [PubMed: 19458720]
5. Andersen ES, Dong M, Nielsen MM, Jahn K, Subramani R, Mamdouh W, Golas MM, Sander B, Stark H, Oliveira CLP, Pedersen JS, Birkedal V, Besenbacher F, Gothelf KV, Kjems J. Nature. 2009; 459:73. [PubMed: 19424153]
6. Ke YG, Douglas SM, Liu MH, Sharma J, Cheng AC, Leung A, Liu Y, Shih WM, Yan H. J Am Chem Soc. 2009; 131:15903. [PubMed: 19807088]
7. Dietz H, Douglas SM, Shih WM. Science. 2009; 325:725. [PubMed: 19661424]
8. Kuzuya A, Komiyama M. Chem Commun. 2009:4182.
9. Endo M, Katsuda Y, Hidaka K, Sugiyama H. J Am Chem Soc. 2010; 132:1592. [PubMed: 20078043]
10. Lund K, Manzo AJ, Dabby N, Michelotti N, Johnson-Buck A, Nangreave J, Taylor S, Pei RJ, Stojanovic MN, Walter NG, Winfree E, Yan H. Nature. 2010; 465:206. [PubMed: 20463735]
11. Voigt NV, Torring T, Rotaru A, Jacobsen MF, Ravnsbaek JB, Subramani R, Mamdouh W, Kjems J, Mokhir A, Besenbacher F, Gothelf KV. Nat Nanotechnol. 2010; 5:200. [PubMed: 20190747]
12. Rinker S, Ke YG, Liu Y, Chhabra R, Yan H. Nat Nanotechnol. 2008; 3:418. [PubMed: 18654566]
13. Kuzuya A, Kimura M, Numajiri K, Koshi N, Ohnishi T, Okada F, Komiyama M. ChemBioChem. 2009; 10:1811. [PubMed: 19562789]
14. Kuzyk A, Laitinen KT, Torma P. Nanotechnology. 2009:20.
15. Ke YG, Lindsay S, Chang Y, Liu Y, Yan H. Science. 2008; 319:180. [PubMed: 18187649]
16. Subramanian HKK, Chakraborty B, Sha R, Seeman NC. Nano Lett. 2011; 11:910. [PubMed: 21235216]
17. Kodera N, Yamamoto D, Ishikawa R, Ando T. Nature. 2010; 468:72. [PubMed: 20935627]
18. Sannohe Y, Endo M, Katsuda Y, Hidaka K, Sugiyama H. J Am Chem Soc. 2010; 132:16311. [PubMed: 21028867]
19. Steinhauer C, Jungmann R, Sobey TL, Simmel FC, Tinnefeld P. Angew Chem, Int Ed. 2009; 48:8870.
20. Glasgow I, Batton J, Aubry N. Lab Chip. 2004; 4:558. [PubMed: 15570365]
21. Howell PB, Mott DR, Fertig S, Kaplan CR, Golden JP, Oran ES, Ligler FS. Lab Chip. 2005; 5:524. [PubMed: 15856089]
22. Mei Q, Xia Z, Xu F, Soper SA, Fan ZH. Anal Chem. 2008; 80:6045. [PubMed: 18593194]
23. Stroock AD, Dertinger SKW, Ajdari A, Mezic I, Stone HA, Whitesides GM. Science. 2002; 295:647. [PubMed: 11809963]
24. Bienvenue JM, Duncalf N, Marchiarullo D, Ferrance JP, Landers JP. J Forensic Sci. 2006; 51:266. [PubMed: 16566759]
25. Chen X, Cui DF, Liu CC, Li H, Chen J. Anal Chim Acta. 2007; 584:237. [PubMed: 17386610]
26. Kim J, Jang SH, Jia GY, Zoval JV, Da Silva NA, Madou MJ. Lab Chip. 2004; 4:516. [PubMed: 15472738]
27. McClain MA, Culbertson CT, Jacobson SC, Allbritton NL, Sims CE, Ramsey JM. Anal Chem. 2003; 75:5646. [PubMed: 14588001]
28. Mun BP, Jung SM, Yoon SY, Kim SH, Lee JH, Yang S. Microfluid Nanofluid. 2010; 8:695.
29. Schilling EA, Kamholz AE, Yager P. Anal Chem. 2002; 74:1798. [PubMed: 11985310]
30. Das C, Zhang J, Denslow ND, Fan ZH. Lab Chip. 2007; 7:1806. [PubMed: 18030404]
31. Fan R, Vermesh O, Srivastava A, Yen BKH, Qin LD, Ahmad H, Kwong GA, Liu CC, Gould J, Hood L, Heath JR. Nat Biotechnol. 2008; 26:1373. [PubMed: 19029914]
32. Hatch AV, Herr AE, Throckmorton DJ, Brennan JS, Singh AK. Anal Chem. 2006; 78:4976. [PubMed: 16841920]
33. Hellmich W, Pelargus C, Leffhalm K, Ros A, Anselmetti D. Electrophoresis. 2005; 26:3689. [PubMed: 16152668]
34. Barton GM, Medzhitov R. Proc Natl Acad Sci USA. 2002; 99:14943. [PubMed: 12417750]
35. Mitchell P. Nat Biotechnol. 2001; 19:1013. [PubMed: 11689841]

36. Palanca-Wessels MC, Barrett MT, Galipeau PC, Rohrer KL, Reid BJ, Rabinovitch PS. Gastroenterology. 1998; 114:295. [PubMed: 9453489]

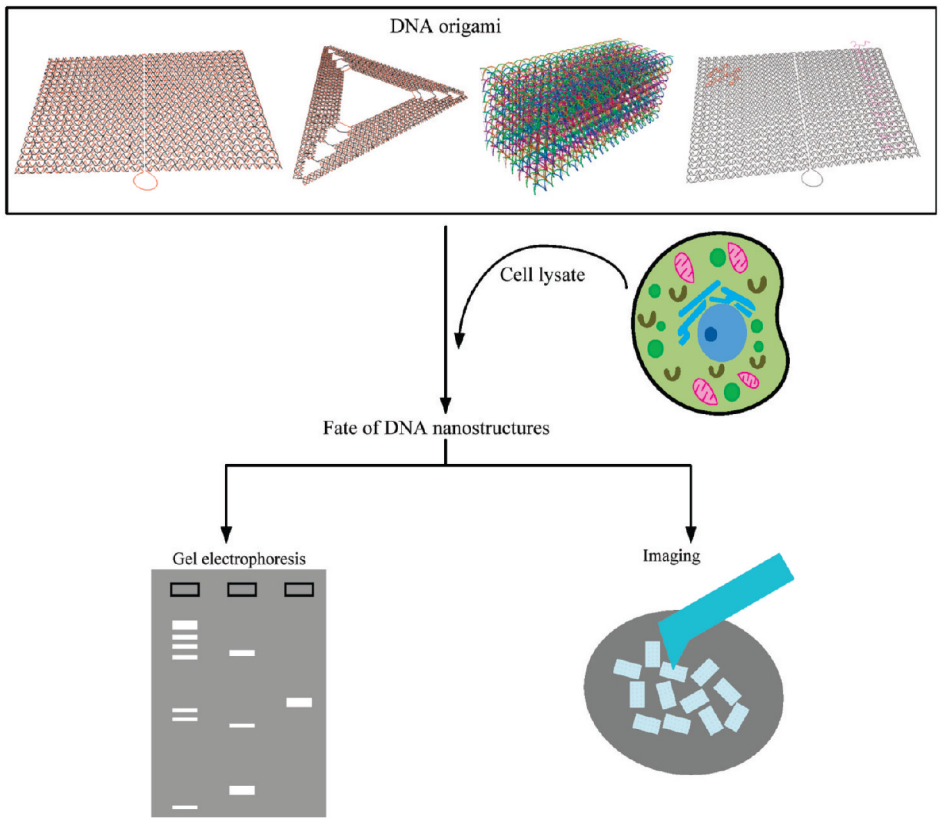


**Figure 1.**
Investigating the fate of DNA nanostructures in cell lysate.

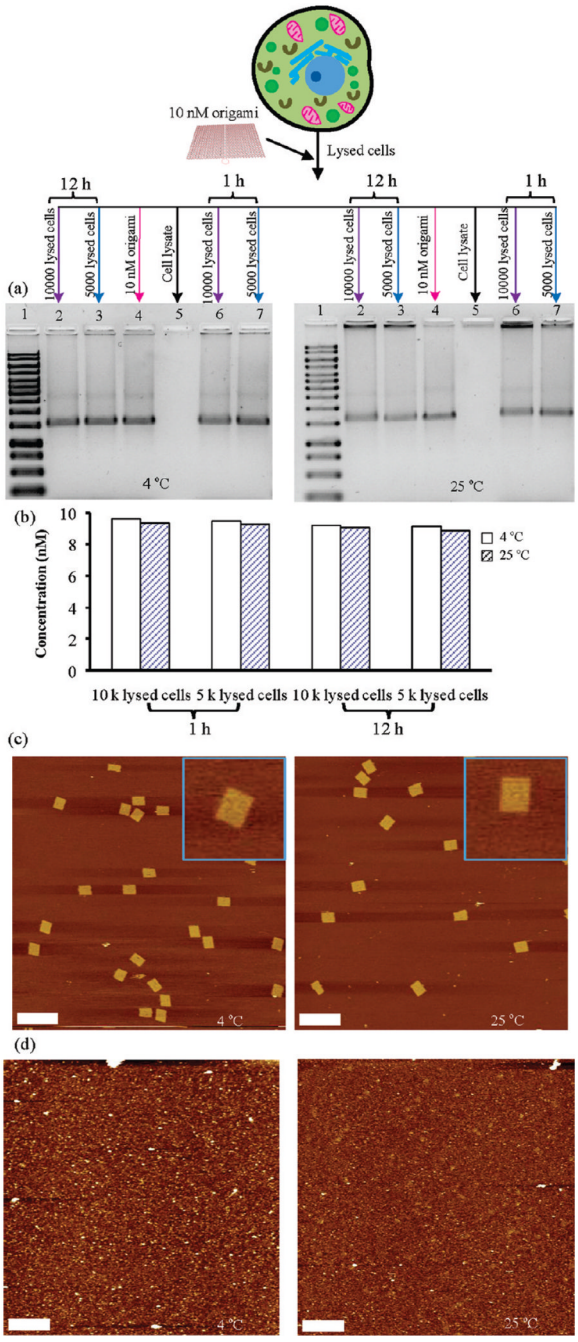


**Figure 2.**

Analysis of rectangular DNA origami stability in, and separability from, CP-A cell lysate. (a) Agarose gels separate origami after incubation at 4 and 25 °C: lane 1, 1000 bp DNA ladder; lane 2, 10000 lysed cells with origami incubated for 12 h; lane 3, 5000 lysed cells with origami incubated for 12 h; lane 4, 10 nM origami; lane 5, cell lysate only; lane 6, 10000 lysed cells with origami incubated for 1 h; lane 7, 5000 lysed cells with origami incubated for 1 h. (b) Concentration of origami products after separation from cell lysate, estimated from the relative band intensities, compared to the control sample in lane 4. (c) Topographic images of rectangular DNA origami extracted from agarose gels. Scale bar = 300 nm (image insets in upper corners are 250 nm by 250 nm). (d) AFM images of origami/

cell lysate mixtures without gel electrophoretic separation, at 4 and 25 °C. Scale bar = 300 nm.

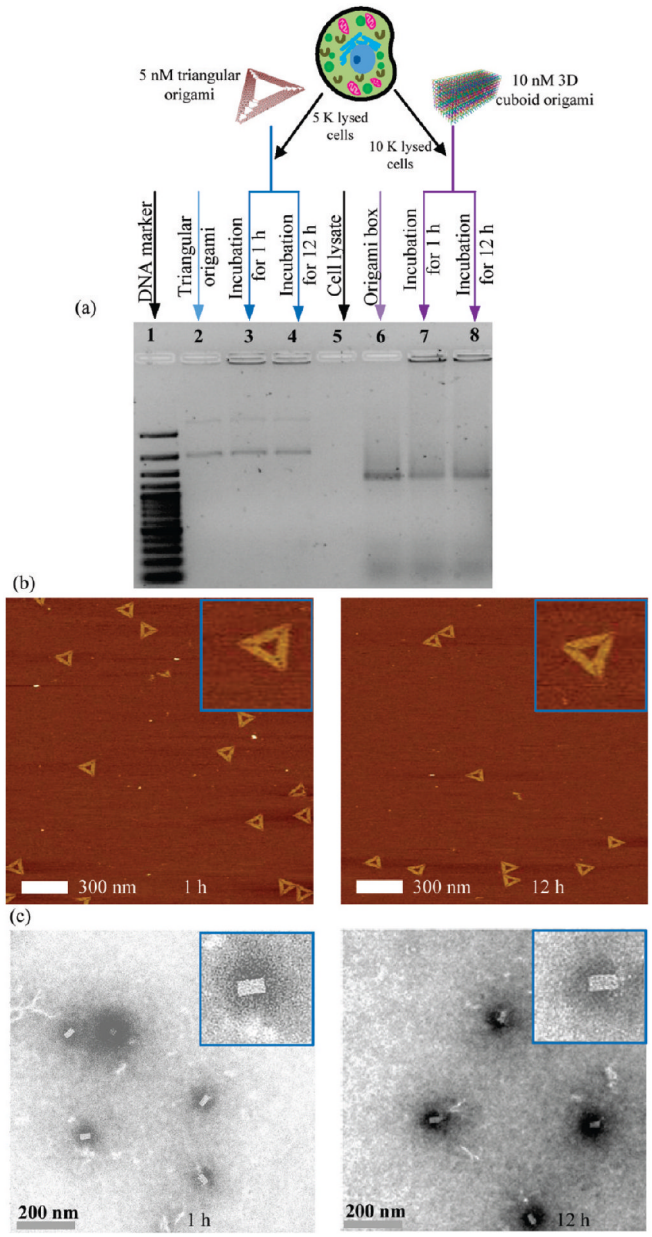


**Figure 3.**

Stability of different origami shapes in CP-A cell lysate. (a) Agarose gel electrophoresis of 2D triangular origami and 3D cuboid origami after incubation with CP-A cell lysate: lane 1, 1 kbp DNA ladder; lane 2, 5 nM triangular origami; lanes 3 and 4, triangular origami incubated with cell lysate for 1 and 12 h; lane 5, cell lysate; lane 6, 10 nM origami cube; lanes 7 and 8, 10 nM origami cube incubated with cell lysate for 1 and 12 h. (b) AFM images of triangular DNA origami after separation from CP-A lysate. Images insets are 250 nm by 250 nm. (c) TEM images of 3D cuboid origami after separation from CP-A lysate. Images insets are 125 nm by 125 nm.

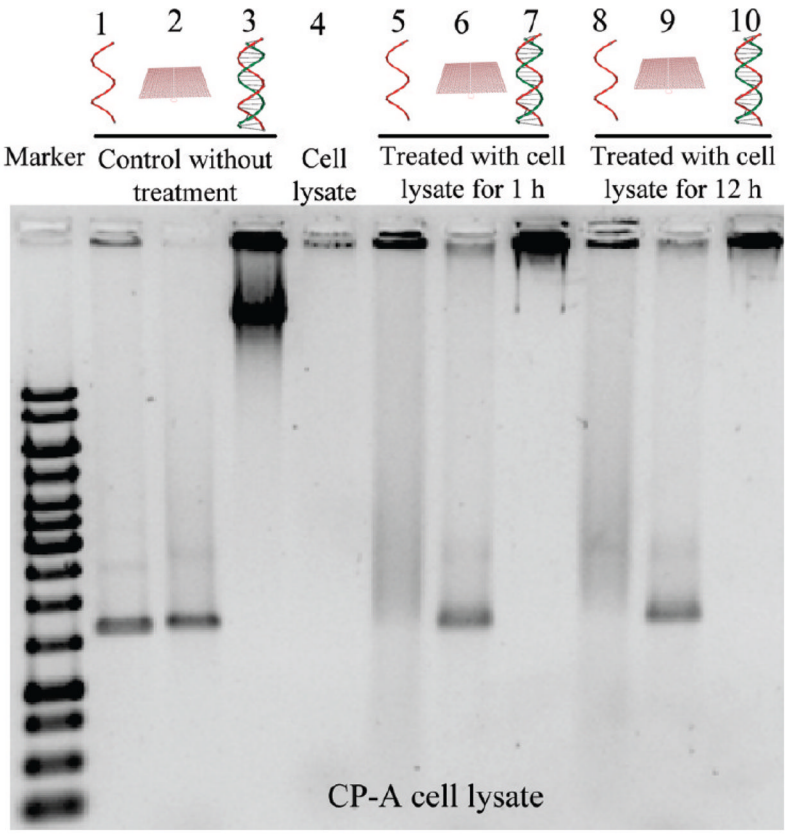


**Figure 4.**

Relative stabilities of rectangular origami, single-stranded M13 viral DNA and double-stranded λ DNA in CP-A cell lysate. Agarose gel electrophoresis confirms that only origami is separable from cellular debris: lane 1, 10 nM M13; lane 2, 10 nM origami; lane 3, 25 ng/μL λ DNA; lane 4, cell lysate; lanes 5–7, M13, origami and λ DNA incubated with cell lysate for 1 h at 25 °C, respectively; lanes 8–10, M13, origami, and λ DNA incubated with cell lysate for 12 h at 25 °C, respectively.

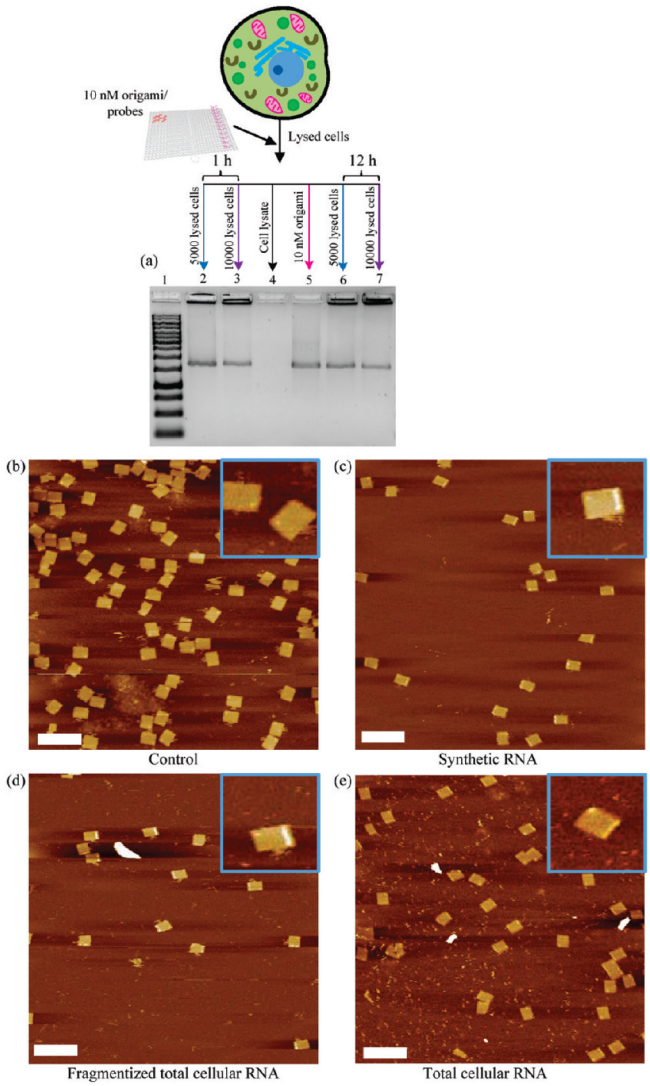


**Figure 5.**

Functional assay of single-stranded probe-bearing DNA origami nanostructure after mixing with HeLa cell lysate. (a) Each DNA origami carries a line of probes positioned near the right edge and is recovered after incubation with HeLa cell lysate using agarose gel: lane 1, 1 kbp DNA ladder; lane 2, 5000 lysed cells with probe bearing DNA origami incubated for 1 h; lane 3, 10000 lysed cells with probe bearing DNA origami incubated for 1 h; lane 4, cell lysate only; lane 5, 10 nM probe bearing DNA origami; lane 6, 5000 lysed cells with probe bearing DNA origami incubated for 12 h; lane 7, 10000 lysed cells with probe bearing DNA origami incubated for 12 h. (b–e) Topographic AFM images of the DNA origami with three different targets after separation from HeLa cel lysate. (b) Control probes mixed with synthetic RNA target. (c) Binding to synthetic RNA. (d) Binding to fragmentized total cellular RNA. (d) Binding to total cellular RNA. Scale bar = 300 nm (image insets are 250 nm by 250 nm).